



Research paper

The characterisation of the “X” crystal structure in the Stillinger-Weber potential



Domagoj Fijan, Mark Wilson*

Department of Chemistry, Physical and Theoretical Chemistry Laboratory, University of Oxford, South Parks Road, Oxford OX1 3QZ, UK

ARTICLE INFO

Article history:

Received 8 June 2017

In final form 30 July 2017

Available online 31 July 2017

ABSTRACT

A recently observed crystal structure is characterised by reference to the calculated diffraction patterns. The “X” crystal is related to the β -Sn crystal structure via an atom displacement and a reduction in symmetry from tetragonal to orthorhombic. A further crystal polymorph is identified which retains the tetragonal symmetry of the β -Sn structure but involves a related atom displacement. The unit cells and space groups are reported. The two crystals are labelled as o-X and t-X respectively. The transformation mechanisms from the β -Sn crystal structure to the two structures are identified. No routes to these crystals from other polymorphs are found.

© 2017 Published by Elsevier B.V.

1. Introduction

There has been enormous levels of experimental and theoretical effort devoted to probing the phase behaviour of systems dominated by local tetrahedral environments under ambient conditions. Systems such as Si and Ge appear homologous in that (broadly speaking) their phase diagrams map onto each other. Both have been studied extensively under pressure (see, for example, Refs. [24,3,12,19,10,14,16,5,29,17,7]) uncovering a rich tapestry of inter-related crystal structures. Computer simulation offers an alternative method for exploring the phase space both as a function of temperature and pressure (and hence mimicking direct experimental study) and as a function of the potential model itself (see, for example, Refs. [20,22,15]). The latter, although not experimentally reproducible, offers the potential to “connect” different (related) systems and to develop a fundamental understanding of the key interatomic interactions.

Whilst electronic structure methods [9] offer potentially the most accurate results (and, by construction, may include any major changes in electronic structure) relatively simple potential models, in which the system energy is expressed as a function of the atom positions, offer a flexible and efficient method for exploring the morphology space. Recent investigations have uncovered yet more complexity and richness in the phase diagrams of silicon and the related mono-water (mW) models [21]. These models employ a Stillinger-Weber (SW) potential in which the system energy is effectively expressed as the sum of 2- and 3-body terms [28].

The 3-body term acts to effectively bias the system against generating local coordination environments which deviate away from ideal tetrahedral angles. Altering the balance between the 2- and 3-body terms has been shown to give a good representation of Si [28], Ge [6] and even H₂O [21].¹ The result is that, under ambient conditions, the diamond crystal structure is energetically favourable. As the pressure is increased, for example, the balance between the 2- and 3-body terms changes and alternative crystal structures may become thermodynamically stable. Romano et al. [27] explored the relative energetics of ~30 different crystal structures for both the Si and mW SW potentials. They showed how the SC16 crystal structure (space group $Pa\bar{3}$ - #205) dominates the high pressure region of the phase diagrams.

Overall, therefore, a full understanding of the phase diagrams of systems such as Si and Ge is still potentially lacking.

2. The “X” crystal

In recent work the phase diagram for the SW potential was determined at positive pressures for a range of different balances between the 2- and 3-body interactions (different values of λ) [2]. These investigations uncovered a potential new phase (termed “X” in the original paper²) which formed spontaneously from a β -Sn

¹ In the SW potential the magnitude of the 3-body interaction is controlled by a parameter usually identified as λ . For example, models for Si, Ge and water use $\lambda = 21$, 20 and 23.15 respectively.

² This is somewhat unfortunate in that, for silicon, Si-X is classified as FCC, which is thermodynamically stable at high pressures. Here we adopt the nomenclature t-X and o-X to denote crystals formed from the β -Sn crystal structure with tetragonal and orthorhombic symmetry respectively.

* Corresponding author.

E-mail address: mark.wilson@chem.ox.ac.uk (M. Wilson).

crystal structure when simulated at $\lambda = 20.08$. The formed X-crystal appears stable at intermediate pressures (between 0.2 and 0.8 in reduced units) and low temperatures (between 0 and 0.02 in reduced units) where the β -Sn crystal structure was previously expected to dominate. Although the static structure factor was reported no attempt was made to characterize the polymorph further. In this Letter we will characterize the new crystal structure and establish its relationship with other known stable crystals including potential (atomistic) transformation mechanisms both into and out of the new structure.

3. Characterization of the “X” crystal structure

3.1. Determination of the space group and primitive cell

A super cell was constructed from $5 \times 5 \times 10$ primitive cells of the β -Sn crystal structure (giving a total of 1000 atoms) at the equilibrium cell lengths for $p^* = 0.26$ and $T^* = 0.01$ (corresponding to $b = a = 4.88 \text{ \AA}$ and $c/a = 0.57$). Molecular dynamics (MD) simulations were performed at constant stress (allowing the cell lengths and angles to vary) using the SW potential with $\lambda = 20.08$ using LAMMPS [25] at $T^* = 0.01$ and $p^* = 0.26$. The phase space point $T^* = 0.01$ and $p^* = 0.26$ corresponds to $p = 10 \text{ GPa}$ and $T = 250 \text{ K}$ for silicon and $P = 7.81 \text{ GPa}$ and $T = 225 \text{ K}$ for germanium. It should be noted that the value of the parameter λ considered lies between values used previously to model germanium and silicon. Further work will be required to explore the model parameter space to establish the potential stable phase space range for related materials such as H_2O and C. The state variables were controlled using Nosé-Hoover [23,13] thermostats and barostats [18] respectively. The initial atom velocities were selected from a Maxwell-Boltzmann distribution with each atom assigned a random velocity vector. Simulations were then performed starting from different sets of initial velocities.

At this state point the β -Sn crystal structure is seen to evolve to two new (related) structures. The initial β -Sn crystal structure is equilibrated over 50,000 time steps with time step of 0.383 fs (corresponding to $\sim 19.15 \text{ ps}$) with a further 100,000 time steps ($\equiv 38.3 \text{ ps}$) performed in the NVT ensemble. The energy of the final structure was minimised using the Polak-Ribiere version of the conjugate gradient method with an energy tolerance of 10^{-4} and force tolerance of 0.97×10^{-6} (reduced units) with a maximum of 1000 iterations and 100,000 force/energy evaluations.

The final (energy minimised) configuration was used as the input into the *spglib* library [1,11] to determine the primitive cell and space group with tolerances in the cell lengths and atom positions of 0.2 \AA . The space group of one of the new structures was found to be Pnma (#62) and is orthorhombic with basis vectors $a = 5.00452 \text{ \AA}$, $b = 4.73424 \text{ \AA}$ and $c = 2.75783 \text{ \AA}$ giving $c/a = 0.551$ $c/b = 0.583$. The primitive cell (in fractional coordinates) is:

x	y	z
0.0	0.13872	0.00000
0.50000	0.500	0.50000
0.0	0.63872	0.26290
0.50000	0.000	0.76290

The primitive cell is closely related to that for the β -Sn crystal structure (space group $\text{I4}_1/\text{amd}$), which has fractional coordinates:

x	y	z
0.0	0.0	0.00
0.5	0.5	0.50
0.0	0.5	0.25
0.5	0.0	0.75

as

x	y	z
0.0	$0.0 + d_y$	0.0
0.5	0.5	0.50
0.0	$0.5 + d_y$	$0.25 + d_z$
0.5	0.0	$0.75 + d_z$

where $d_y = 0.13872$ and $d_z = 0.0129$. Fig. 1(a) shows schematically the changes in both the atom positions and cell geometry on transformation from the β -Sn crystal structure to the o-X structure.

The second phase that can form from β -Sn crystal structure is tetragonal (here termed t-X) and *spglib* predicts the space group P4_12_12 (# 92) with lattice vectors $a = b = 4.88240 \text{ \AA}$ and $c = 2.76938 \text{ \AA}$ giving $c/a = 0.567$ and primitive cell

x	y	z
0.06954	0.00000	0.00000
0.50000	0.43046	0.50000
0.00000	0.50000	0.25000
0.56954	0.93046	0.75000

This is related to the β -Sn crystal structure as follows:

x	y	z
$0.0 + d$	$0.0 + d$	0.00
0.5	0.5	0.50
0.0	$0.5 + d$	0.25
$0.5 + d$	0.0	0.75

where $d = 0.06954$. Fig. 1(b) shows the atoms displacements associated with the change from the β -Sn crystal structure.

In summary, the unit cells of the two new crystals, and their relationship to the originating β -Sn crystal structure, are as follows.

β -Sn			t-X			o-X		
x	y	z	x	y	z	x	y	z
0.0	0.0	0.00	$0.0 + d$	$0.0 + d$	0.00	0.0	$0.0 + d_y$	0.00
0.5	0.5	0.50	0.5	0.5	0.50	0.5	0.5	0.50
0.0	0.5	0.25	0.0	$0.5 + d$	0.25	0.0	$0.5 + d_y$	$0.25 + d_z$
0.5	0.0	0.75	$0.5 + d$	0.0	0.75	0.5	0.0	$0.75 + d_z$

where $d = 0.06954$ and $d_y = 0.13872$, $d_z = 0.0129$. Fig. 1(c) shows the atoms projected onto the xy plane for the β -Sn, t-X and o-X crystal structures. Both the o-X and t-X crystals show the same basic distortions (alternate layers of atoms shifted) with the t-X crystal showing the distortion along both the a and b directions and the t-X crystal showing the distortion only along the a direction.

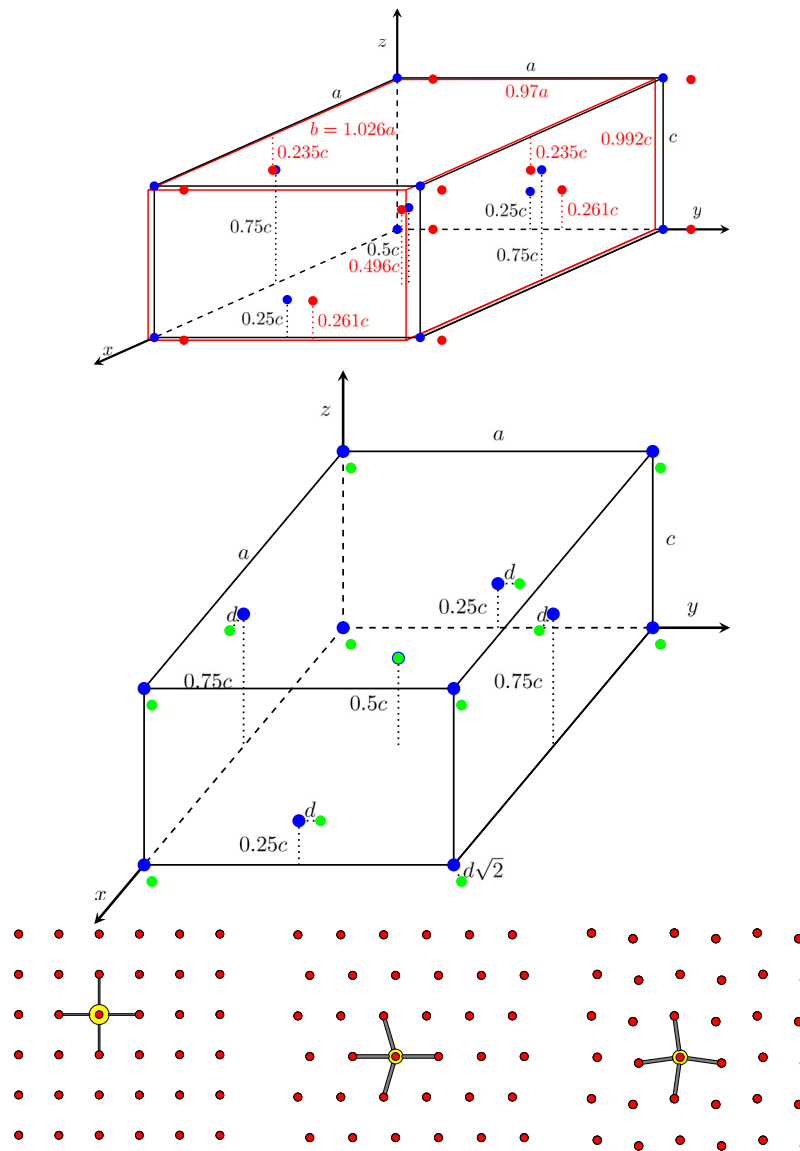


Fig. 1. (a) Changes in unit cell dimensions and geometry on transforming from the β -Sn to o-X crystal structure. The black lines and blue circles highlight the original β -Sn crystal cell whilst the red circles and lines show the resulting o-X cell. (b) Changes in unit cell dimensions and geometry on transforming from the β -Sn to t-X crystal structure. The black lines and blue circles highlight the original β -Sn crystal cell whilst the green circles show the resulting t-X atom positions. The cell geometry is almost unchanged in the transformation. (c) The (left to right) β -Sn, o-X and t-X crystal structures seen along the c direction. The coordination of a single highlighted atom is shown in all three cases. (For interpretation of the references to colour in this figure legend, the reader is referred to the web version of this article.)

3.2. The diffraction pattern

Fig. 2 shows the structure factor, $S(k)$, for key crystal structures; β -Sn, t-X and o-X. The total X-ray scattering function and structure factor are simply related via a (k -dependent) form factor function. Since we are primarily interested in the peak positions (rather than their intensities) then considering $S(k)$ alone is appropriate. The Ashcroft-Langreth structure factors are generated from $S(k) = \langle A^*(k) \cdot A(k) \rangle$, where the Fourier components $A(k) = \frac{1}{\sqrt{N}} \sum_i e^{ik \cdot r_i}$ and $\{r_i\}$ are the atom positions. The X-ray diffraction pattern for the β -Sn crystal structure is well known (see, for example, references [14,16,12,19,10]) showing peaks corresponding to $[hkl] = [200]$, $[101]$, $[220]$, $[221]$, $[301]$, $[112]$, $[400]$ and $[321]$. The sum $h^2 + k^2 + l^2$ is even as expected for this symmetry. For both the t - and o -distortions this constraint is relaxed and a number of additional peaks appear as highlighted. For example, Bragg peaks corresponding to $[120]$, $[111]$, $[201]$, $[221]$ and $[301]$

emerge. On reducing the symmetry from tetragonal to orthorhombic further peaks appear (also as indicated) as $[hkl] \neq [khl]$. For example, the pairs $\{[200]$, $[020]\}$, $\{[101]$, $[011]\}$ and $\{[120]$, $[210]\}$ become distinct. Most importantly, the peak positions for the o-X crystal structure agree with those obtained previously [2] (as shown in the figure inset).

4. Dynamics

4.1. Transformation mechanism

Fig. 3(a) shows the evolution of the simulation cell lengths as the β -Sn crystal structure transforms to either the tetragonal or orthorhombic X-forms. Fig. 3(b) shows the evolution of the system energy and volume for the same transformations mapped onto the (ideal) $T = 0$ K energy/volume curves. The energy/volume curves were calculated by constructing a supercell from the appropriate

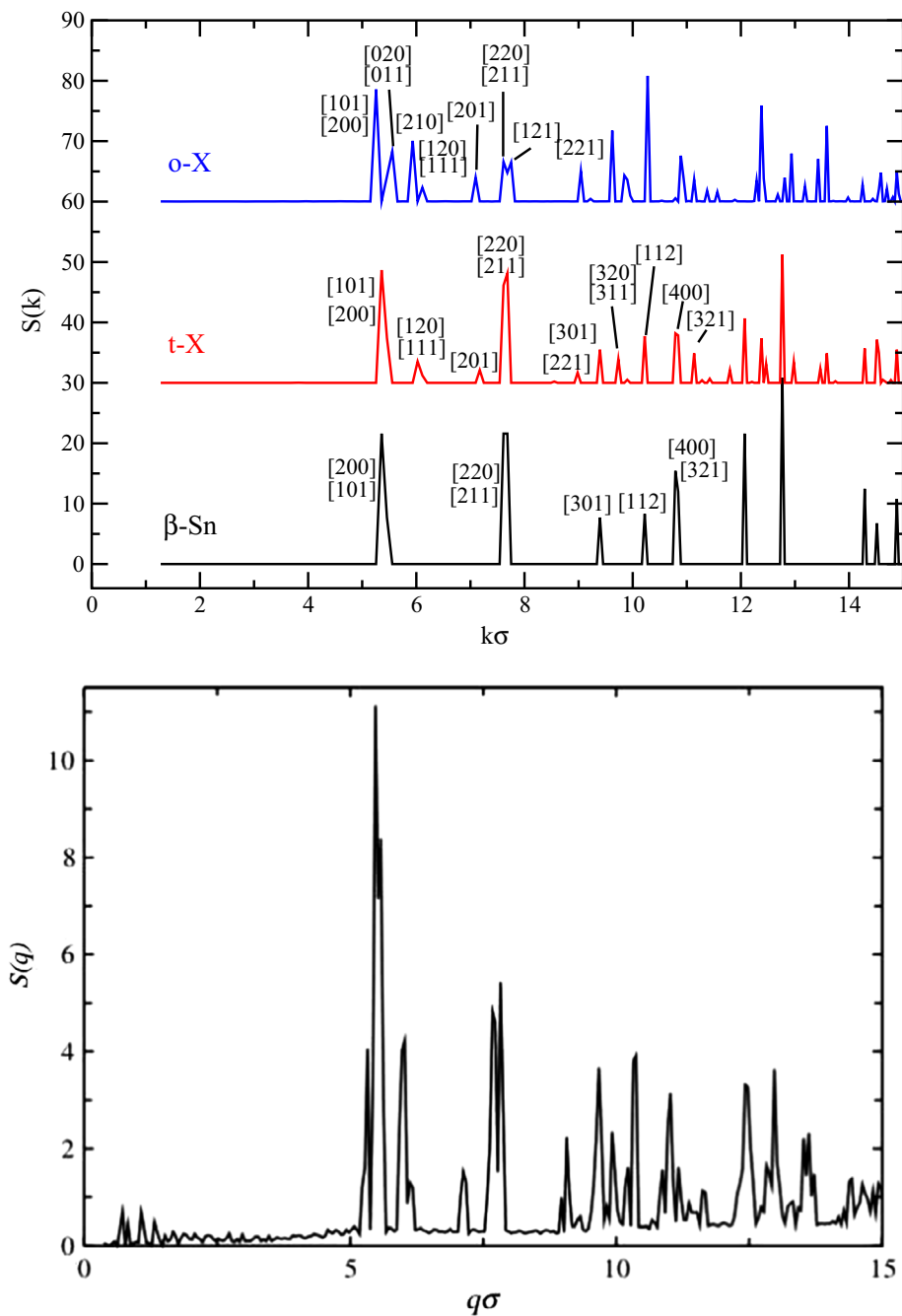


Fig. 2. (a) Static structure factors, $S(k)$, for the β -Sn, t-X and o-X crystal structures shown as a function of reduced k ($\equiv k\sigma$ where $\sigma = 2.0951$ Å). In each case the series of low- k peaks are highlighted as $[hkl]$. As the β -Sn crystal structure transforms to t-X the cell symmetry is reduced and Bragg peaks corresponding to $h^2 + k^2 + l^2 = \text{odd}$ are allowed. As the β -Sn crystal structure transforms to o-X additional peaks emerge as $[hkl] \neq [khl]$. (b) Static structure factor previously observed (from Ref. [2]).

unit cells and performing single point energy calculation. For structures lacking cubic symmetry ($a = b = c$) calculations are performed over a range of c/a and c/b ratios to identify the lowest energy structure. The unit cell volumes were varied by increasing the cell length in steps of 0.02 Å. The transformations from the β -Sn crystal structure originate at the same state point (as noted above) and proceed along analogous UV paths until $U^* \sim -1.92$ and $V^* \sim 1.788$ (both in reduced units). At this state point an effective “bifurcation” occurs with the system heading towards one of the two X forms and commensurate with the changes in cell lengths seen in Fig. 3(a). The pathway to either structure was found to be dependent upon

the distribution of velocities and showed no systematic dependence upon the system cell size (number of unit cells).

Table 1 lists the energies and volumes at the respective energy minima in the $T = 0$ K energy/volume curves. The o-X and t-X crystals are ~ 690 J mol $^{-1}$ more energetically favourable than the β -Sn crystal structure.

The key observation (consistent with that made in Ref. [2]) is that the o-X crystal structure is thermodynamically stable over the β -Sn crystal structure.

Fig. 3(b) also highlights how it is also possible to thermally-drive the transformation from the t- to o-X forms. The t-X crystal

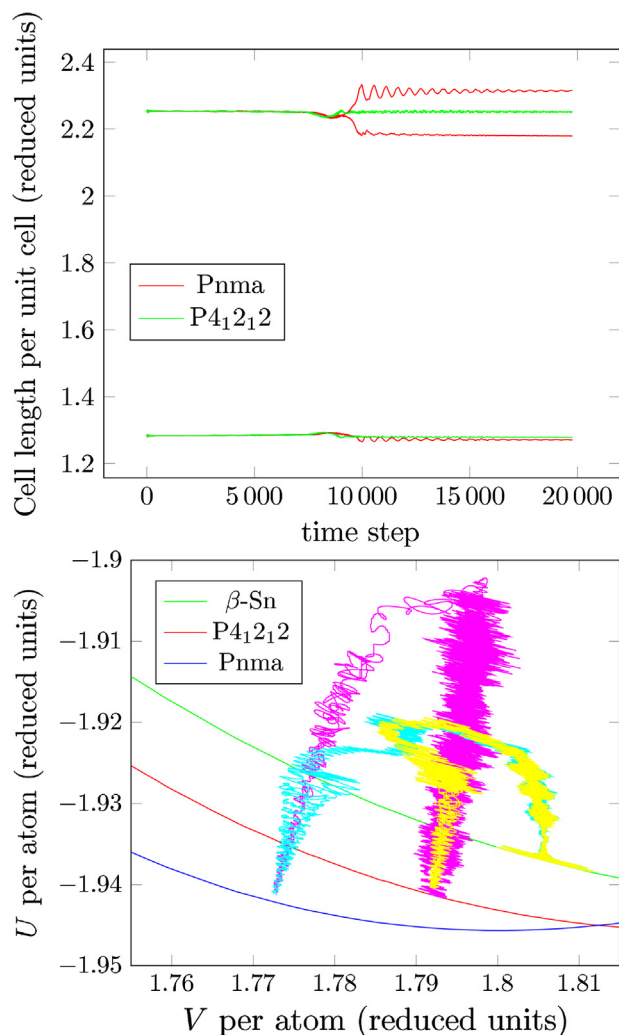


Fig. 3. (a) The evolution of the simulation cell lengths on transformation from the β -Sn crystal structure to both the o-X and t-X forms. The original β -Sn crystals are heated from $T = 10$ K to 250 K at a pressure of $p = 10$ GPa using different distributions of initial velocities. After the phase transformations the system was cooled down to 10 K. (b) Potential energy evolution during the transformations from the β -Sn crystal structure to either the t- or o-X structures, and from the t-X to o-X as described in the text. For the t- to o-X transformation the same procedure as above was used with heating to $T = 550$ K required to drive the transformation. The $T = 0$ K ideal energy/volume curves are overlaid to highlight the transformation pathways.

Table 1

Volumes and energies (expressed in reduced units) for the three key crystal structures (β -Sn, o-X and t-X). The corresponding values for the thermodynamically stable form at ambient conditions, the diamond crystal structure, are shown for comparison.

Crystal	$V^*/\text{reduced units}$	$U^*/\text{reduced units}$
Diamond	2.1746	-2.0000
β -Sn	1.8464	-1.9424
t-X	1.8257	-1.9457
o-X	1.8007	-1.9457

is systematically heated from low temperature with a transformation to the orthorhombic form observed at $T^* \sim 0.22$.

4.2. Attempted transformations to the X phase

It is clear from the above discussion that the β -Sn crystal structure will, under appropriate conditions, transform to either a t-X or o-X structure depending on the atomistic detail of the starting con-

figuration. To investigate potential transformation pathways to the X crystals from other crystal polymorphs, a range of alternative crystal structures (diamond, lonsdaleite, FCC, SC16, ST12 and BC8) were constructed and modelled at a point in phase space where the X crystal is expected to be thermodynamically stable, $p^* = 0.26$, $T^* = 0.01$. The diamond and lonsdaleite crystal structures differ in the stacking of the atomic layers, the former showing cubic stacking and the latter hexagonal stacking (see, for example, Refs. [8,26,4]). Simulations are performed using a SW potential with $\lambda = 20.08$. The only transformation to the X phase which was observed on the simulation time-scale was from the β -Sn crystal structure. The diamond, lonsdaleite, SC16, and ST12 crystal structures are all metastable at this state point. The BC8 crystal transformed to the SC16 crystal structure as seen previously [27].

4.3. Attempted transformations from the X phase

In addition to considering the transformation to the X phase potential transformations away from this polymorph are also considered. Ideal t-X and o-X crystals (both corresponding to $5 \times 5 \times 10$ unit cells) are constructed and MD simulations are performed over a range of state points at which the X crystals would be anticipated as metastable and at which the diamond and SC16 crystal structures would be expected to be thermodynamically stable. Simulations are performed starting from the state point $p^* = 0.26$, $T^* = 0.01$ both along the isotherm and the isochore. As the system is heated along the isochore the transformations between the crystal structures t-X \rightarrow o-X \rightarrow β -Sn are observed at $T^* = 0.0189$ and 0.0298 respectively. In addition, both the t-X and o-X structures, pressurised along the isotherm, form the β -Sn crystal structure at $p^* = 1.826$ with the t-X structure undergoing a transformation to the o-X at $p^* = 0.476$. On de-pressurisation along the isotherm the o-X crystal transforms to the β -Sn crystal structure (at $p^* = -0.15$) whilst the t-X remains metastable to $p^* \sim -0.20$. The system shows the expected hysteresis which would likely be strongly system size dependent. Overall, therefore, both the o-X and t-X structures readily transform to the β -Sn crystal structure which remains metastable under the conditions tested.

5. Conclusions

In this letter the previously observed “X” crystal [2] has been fully characterised by reference to the diffraction patterns. The crystal structure is related to the β -Sn crystal structure via a simple atom displacement and a reduction in cell symmetry from tetragonal to orthorhombic (and is termed o-X here). A related distortion, in which the tetragonal cell symmetry is maintained, has also been observed (leading to the so-called t-X crystal structure). Finally, the accessibility of this crystal structure from potential crystalline polymorphs was considered with the route from the β -Sn crystal structure identified as unique.

Acknowledgements

DF is grateful to St. Edmund Hall and the Clarendon Fund (University of Oxford) for financial support. We are grateful for support from the EPSRC Centre for Doctoral training, Theory and Modelling in Chemical Sciences, under grant EP/L015722/1. This paper conforms to the RCUK data management requirements.

References

- [1] P.D. Adams, Algorithms for deriving crystallographic space-group information. II. Treatment of special positions research papers, *Acta Crystallogr. Sect. A: Found. Crystallogr.* 58 (2002) 60–65.

- [2] K. Akahane, J. Russo, H. Tanaka, A possible four-phase coexistence in a single-component system, *Nat. Commun.* 7 (2016) 12599.
- [3] A. Mujica, A. Rubio, A. Munoz, R.J. Needs, *Rev. Mod. Phys.* 75 (2003) 863.
- [4] A.P. Jones, P.F. McMillan, C.G. Salzmann, M. Alvaro, F. Nestola, M. Prencipe, D. Dobson, R. Hazael, M. Moore, *Lithos* 265 (2016) 214.
- [5] B.D. Malone, M.L. Cohen, *Phys. Rev. B* 85 (2012) 024116.
- [6] M.H. Bhat, V. Molinero, V. Soignard, V.C. Solomon, S. Sastry, J.L. Yarger, C.A. Angell, Vitrification of a monatomic metallic liquid, *Nature* 448 (7155) (2007) 787–790.
- [7] C.C. Yang, J.C. Li, Q. Jiang, *Sol. State Commun.* 129 (2004) 437.
- [8] C.G. Salzmann, B.J. Murray, J.J. Shephard, *Diamond Related Mater.* 59 (2015) 69.
- [9] C.J. Pickard, R.J. Needs, *Phys. Stat. Solidi B* 246 (2009) 536.
- [10] G.A. Voronin, C. Pantea, T.W. Zerda, L. Wang, Y. Zhao, *Phys. Rev. B* 68 (2003) 020102(R).
- [11] N. Haven, Algorithms for deriving crystallographic space-group information, *Acta Crystallogr. Sect. A: Found. Crystallogr.* 55 (1999) 383–395.
- [12] H. Olijnyk, S.K. Sikka, W.B. Holzapfel, *Phys. Lett.* 103A (1984) 137.
- [13] W.G. Hoover, Canonical dynamics: equilibrium phase-space distributions, *Phys. Rev. A* 31 3 (1985) 1695–1697.
- [14] J. Jamieson, *Science* 139 (1963) 762.
- [15] J. Behler, R. Martonak, D. Donadio, M. Parrinello, *Phys. Rev. Lett.* 100 (2008) 185501.
- [16] J.Z. Hu, I.L. Spain, *Solid State Commun.* 51 (1984) 263.
- [17] J.Z. Hu, L.D. Merkle, C.S. Menoni, I.L. Spain, *Phys. Rev. B* 34 (1986) 4679.
- [18] G.J. Martyna, D.J. Tobias, M.L. Klein, *J. Chem. Phys.* 101 (1994) 4177.
- [19] M.I. McMahon, R.J. Nelmes, *Phys. Rev. B* 47 (1993) 8337.
- [20] M. Kaczmariski, O.N. Bedoya-Martinez, E.R. Hernandez, *Phys. Rev. Lett.* 94 (2005) 095701.
- [21] V. Molinero, E.B. Moore, Water modeled as an intermediate element between carbon and silicon, *J. Phys. Chem. B* 113 (13) (2009) 4008–4016.
- [22] M. Wilson, P.F. McMillan, *Phys. Rev. Lett.* 90 (2003) 135703.
- [23] S. Nosé, A unified formulation of the constant temperature molecular dynamics methods, *J. Chem. Phys.* 81 1 (1984) 511–519.
- [24] P.F. McMillan, *Nat. Mat.* 1 (2002) 19.
- [25] S. Plimpton, Fast parallel algorithms for short - range molecular dynamics, *J. Comput. Phys.* 117 (June 1994) (1995) 1–19.
- [26] P. Nemeth, L.A.J. Garvie, T. Aoki, N. Dubrovinskaia, L. Dubrovinsky, P.R. Buseck, *Nat. Commun.* 5 (2014) 5447.
- [27] F. Romano, J. Russo, H. Tanaka, Novel stable crystalline phase for the Stillinger-Weber potential, *Phys. Rev. B Condens. Matter* 90 (2014) 014204.
- [28] F.H. Stillinger, T.A. Weber, Computer simulation of local order in condensed phases of silicon, *Phys. Rev. B* 31 8 (1985) 5262–5271.
- [29] Z. Zhao, F. Tian, X. Dong, Q. Li, Q. Wang, H. Wang, X. Zhong, B. Xu, D. Yu, J. He, H.-T. Wang, Y. Ma, Y. Tian, *J. Am. Chem. Soc.* 134 (2012) 12362.